Interaction of Model Class A_1, Class A_2, and Class Y Amphipathic Helical Peptides with Membranes†

Vinod K. Mishra* and Mayakonda N. Palgunachari

Departments of Medicine and Biochemistry, Atherosclerosis Research Unit, University of Alabama at Birmingham Medical Center, Birmingham, Alabama 35294

Received March 29, 1996; Revised Manuscript Received June 24, 1996⊗

ABSTRACT: To test the hypothesis that differences in the lipid affinity of exchangeable apolipoproteins are due to the presence of different classes of amphipathic α-helical motifs which differ primarily in the distribution of charged amino acid residues, we designed and synthesized model peptides mimicking class A_1, class A_2, and class Y amphipathic helices present in these apolipoproteins. Both class A_1 and class A_2 helices have positive residues at the polar−nonpolar interface and negative residues at the center of the polar face. However, clustering of positive and negative residues is less exact in class A_1 compared to class A_2 helices. The class Y helices have two negative residue clusters on the polar face separating the two arms and the base of the Y motif formed by three positive residue clusters. The lipid affinities of three 18 residue model peptides representing these classes, Ac-18A_1-NH_2 (Ac-ELLEKWAEK-LAALKEALK-NH_2), Ac-18A_2-NH_2 (Ac-ELLEKWKEALAALAEKLK-NH_2), and Ac-18Y-NH_2 (Ac-ELLKAWKEALEALKEKLA-NH_2), were determined by right-angle light scattering, circular dichroism spectroscopy, differential scanning calorimetry, and fluorescence spectroscopy. The observed rank order of lipid affinity of these three peptides is: Ac-18A_2-NH_2 > Ac-18Y-NH_2 > Ac-18A_1-NH_2. This order is consistent with the known lipid affinity of exchangeable apolipoproteins containing class A_1, class A_2, and class Y helices (class A_2 > class Y > class A_1). Results of this study illustrate the important role of interfacial lysine residues in modulating the lipid affinity of amphipathic helices and suggest that the effect of interfacial lysine residues in increasing lipid affinity is additive. We propose that interfacial lysine residues, in addition to widening the hydrophobic face because of snorkeling, also help anchor the amphipathic helix in the lipid bilayer.

Lipoproteins are molecular complexes of lipids and proteins. Lipoproteins play an exceedingly important role in the cellular metabolism of lipids by serving as vehicles for transporting lipids and other lipid-soluble molecules in the bloodstream. Apolipoproteins present in the lipoproteins have been broadly classified into two groups, namely, exchangeable apolipoproteins (apo[1] A-I, A-II, A-IV, C-I, C-II, C-III, and E) and nonexchangeable apolipoproteins (apo B-100 and B-48). The exchangeable apolipoproteins are able to exchange between different lipoprotein particles during the lipid metabolism, whereas nonexchangeable apolipoproteins do not. The structural and functional properties of apolipoproteins have been summarized in recent review articles (Weisgraber, 1994; Brouillette & Anantharamaiah, 1995; Rosseneu & Labeur, 1995). The exchangeable apolipoproteins were postulated to contain several amphipathic helices which facilitate their binding to the lipids (Segrest et al., 1974). There is now a large body of experimental evidence to support that the amphipathic helices in the exchangeable apolipoproteins are involved in lipid association (Jonas, 1992; Anantharamaiah et al., 1993; Segrest et al., 1994).

The amphipathic helices present in biologically important peptides and proteins have been grouped into several different classes based on their physical−chemical and structural properties (Segrest et al., 1990). The distribution of charged amino acid residues in the polar face of the helix is the predominant difference among different classes of amphipathic helices. The amphipathic helices present in exchangeable apolipoproteins belong to class A in the above classification (Segrest et al., 1990). The class A amphipathic helices are characterized by the presence of positively charged amino acid residues at the polar−nonpolar interface and negatively charged amino acid residues at the center of the polar face. A detailed computer analysis of all the class A amphipathic helices present in exchangeable apolipoproteins revealed that the distribution of positive and negative residues is not identical in all of them. Furthermore, it was observed that even in a given apolipoprotein, amphipathic helices differ in the distribution of charged amino acid residues. It is known that the lipid affinity of different exchangeable apolipoproteins varies appreciably (Sparrow & Gotto, 1982; Pownall & Massey, 1982; Jonas, 1992;

† This work was supported in part by NIH Program Project grant HL34343. V.K.M. is a recipient of Postdoctoral National Research Service Award HL 07631-07

* To whom correspondence should be addressed at D640, 1808 Seventh Ave. S., UAB Medical Center, Birmingham, AL 35294-0012. Phone: (205) 934-1883. FAX: (205) 975-8079. E-mail: vinod@aru.dom.uab.edu.

⊗ Abstract published in *Advance ACS Abstracts,* August 15, 1996.

[1] Abbreviations: apo, apolipoprotein; HDL, high-density lipoprotein(s); DMPC, 1,2-dimyristoyl-*sn*-glycero-3-phosphocholine; POPC, 1-palmitoyl-2-oleoyl-*sn*-glycero-3-phosphocholine; (*n*,*n*+1)-diBrPC, 1-palmitoyl-2-stearoyl-(*n*,*n*+1)-dibromo-*sn*-glycero-3-phosphocholine; NATA, *N*-acetyltryptophanamide; TFE, 2,2,2-trifluoroethanol; Ac, acetyl; NH_2, amide; RP-HPLC, reversed-phase high-performance liquid chromatography; TFA, trifluoroacetic acid; MLVs, multilamellar vesicles; SUVs, small unilamellar vesicles; CD, circular dichroism; DSC, differential scanning calorimetry.

S0006-2960(96)00760-X CCC: $12.00

Anantharamaiah et al., 1993). For instance, it is known that apolipoprotein A-I can be displaced by apolipoprotein A-II from high-density lipoproteins (HDL) because of higher lipid affinity of apolipoptotein A-II compared to apolipoprotein A-I (Jonas, 1992). Also, the different amphipathic helical segments in a given apolipoprotein have different lipid affinity (Sparrow & Gotto, 1980; Palgunachari et al., 1996). It is likely, therefore, that the exact distribution of charged amino acid residues modulates the lipid affinity of these amphipathic helices (Segrest et al., 1994).

To understand the molecular basis of differences in the lipid affinity of amphipathic helical domains, a further computer analysis of exchangeable apolipoproteins (apo A-I, A-II, A-IV, C-I, C-II, C-III, and E) was carried out. This analysis revealed the presence of subclasses among the class A amphipathic helices (class A_1, class A_2, and class A_4) as well as other classes, namely, class Y, class G^*, and amphipathic helices present in insect apolipophorin III (Segrest et al., 1992). The distribution of class A_1, class A_2, and class Y helices in apolipoproteins is as follows: apolipoproteins A-I and E (class A_1); apolipoproteins A-II, C-I, C-II, and C-III (class A_2); apolipoproteins A-I and A-IV (class Y). Class A_1, class A_2, and class Y amphipathic helices differ in the distribution of charged amino acid residues and their clustering on the polar face of the helix. In class A_2 amphipathic helices, the midpoints of the positive residue clusters are symmetrically distributed at $\pm 100°$ from the center of the nonpolar face of the helix, and the separation between the positive and negative residue charge clusters is exact (Segrest et al., 1992). In class A_1 helices, the positive residue clusters are distributed at $\pm 90°$ from the center of the nonpolar face, and separation of the positive and negative residue charge clusters is not as exact as in class A_2 helices (Segrest et al., 1992). Class Y helices are characterized by the presence of two negative amino acid residue clusters separating the two arms and the base of the Y motif formed by three positive amino acid residue clusters on the polar face (Segrest et al., 1992). The distribution of charged amino acid residues in class A_1, class A_2, and class Y amphipathic helices present in exchangeable apolipoproteins is illustrated in Figure 1. The number of different classes of amphipathic helices present varies among different apolipoproteins (Segrest et al., 1994). The presence of different classes of amphipathic helices is postulated to modulate the lipid affinity and functional properties of apolipoproteins (Segrest et al., 1992). In the present study, we have determined the lipid affinity of model amphipathic helical peptides which mimic the distribution of charged amino acid residues in class A_1, class A_2, and class Y helices present in exchangeable apolipoproteins.

MATERIALS AND METHODS

Materials. 1,2-Dimyristoyl-*sn*-glycero-3-phosphocholine (DMPC), 1-palmitoyl-2-oleoyl-*sn*-glycero-3-phosphocholine (POPC), and 1-palmitoyl-2-stearoyl-(6−7, 9−10, and 11−12)-dibromo-*sn*-glycero-3-phosphocholine (6−7-diBrPC, 9−10-diBrPC, and 11−12-diBrPC) were purchased from Avanti Polar Lipids, Inc. (Alabaster, AL), and used without further purification. *N*-Acetyltryptophanamide (NATA) was obtained from Novabiochem (La Jolla, CA). Acrylamide (purity >99.9%) was purchased from Bio-Rad Laboratories (Richmond, CA). Triton X-100 was obtained from Fisher Scientific Co. (Orangeburg, NY). (1*S*)-(+)-10-Camphorsulfonic acid (99%), 2,2,2-trifluoroethanol (TFE, 99.5+%, NMR grade), and guanidine hydrochloride (Gdn·HCl, 99%) were obtained from Aldrich Chemical Co. (Milwaukee, WI). All other chemicals were of the highest purity available commercially.

Synthesis and Purification of the Peptides. Peptides Ac-18A_1-NH_2 (Ac-ELLEKWAEKLAALKEALK-NH_2), Ac-18A_2-NH_2 (Ac-ELLEKWKEALAALAEKLK-NH_2) and Ac-18Y-NH_2 (Ac-ELLKAWKEALEALKEKLA-NH_2) were synthesized by the solid phase method using Fmoc-chemistry (Stewart & Young, 1984) as described previously (Palgunachari et al., 1996). The peptides were purified using a C-4 preparative reversed-phase HPLC (RP-HPLC) column (VYDAC, 2.2 cm i.d. × 25 cm, particle size 10 μm) on a Beckman HPLC system. A linear gradient of 10% acetonitrile to 80% acetonitrile (containing 0.1% TFA) in 70 min with a flow rate of 4.8 mL/min was used. Peptide purity was checked by analytical RP-HPLC (Beckman System Gold 166) using a C-18 column (VYDAC, 4.6 mm i.d. × 25 cm, particle size 5 μm) and a linear gradient of 25% acetonitrile to 70% acetonitrile in 45 min with a flow rate of 1.2 mL/min. Peptide identity was confirmed by mass spectral analysis on a PE-Sciox APT-III triple quadruple ion-spray mass spectrometer (Toronto, Canada).

Preparation of Peptide Solutions. Peptides were dissolved in 6 M Gdn·HCl. The solution was dialyzed (1000 MW cutoff dialysis tube; Spectrum, Houston, TX) against phosphate-buffered saline (PBS: 1.47 mM KH_2PO_4, 6.45 mM $Na_2HPO_4 \cdot 7H_2O$, 136.89 mM NaCl, and 2.68 mM KCl, pH 7.4) extensively (overnight, with three buffer changes). All the studies described below were done in the same buffer.

The concentrations were determined by diluting peptide stock solutions in 6 M Gdn·HCl and measuring the absorbance at 280 nm ($\epsilon_{280} = 5600\ M^{-1}\ cm^{-1}$).

Preparation of Lipid Vesicles. Multilamellar vesicles (MLVs) of DMPC were prepared as follows. About 20 mg of lipid was dissolved in 200 μL of chloroform in a test tube. The organic solvent was removed by blowing nitrogen gas over it. The residual solvent was removed by storing the test tube in a vacuum oven under high vacuum at room temperature for 3 h. The thin film of the lipid deposited on the walls of the test tube was hydrated by 10 freeze−thaw cycles using liquid nitrogen and hot water with vigorous vortexing between each cycle. Small unilamellar vesicles (SUVs) of POPC were prepared by sonicating MLVs in a bath sonicator at 4 °C for 6 h. For preparing SUVs containing dibrominated lipids, the latter were codissolved with POPC in the organic solvent followed by evaporation of the organic solvent, hydration, and sonication as described above. Lipid concentrations were determined using the ashing procedure for total phosphate determination (Ames, 1966).

Right-Angle Light Scattering Measurements. The decrease in the scattered light intensity as a function of time due to the solubilization of DMPC MLVs after addition of the peptide was followed using an SLM 8100 photon counting spectrofluorometer (SLM Instruments, Inc., Urbana, IL). Both emission and excitation wavelengths were set at 400 nm. The band-passes were 4 nm. A 200 μM suspension of DMPC MLVs in a total volume of 2 mL was maintained at 25 °C with constant stirring. To the suspension was added 10 μM peptide solution. As a positive control, complete dissolution of MLVs was achieved by adding 600 μM Triton

X-100 to the vesicle suspension. The data were acquired using slow time based acquisition.

Circular Dichroism (CD) Spectroscopy. The CD spectra were recorded with an AVIV 62DS spectropolarimeter (Lakewood, NJ) equipped with a thermoelectric temperature controller and interfaced to a personal computer. The instrument was calibrated with (1*S*)-(+)-10-camphorsulfonic acid (Woody, 1995; Johnson, 1990; Yang et al., 1986). The CD spectra were measured from 260 to 190 nm every 0.5 nm with 1 s averaging per point, and a 2 nm band-pass. An 0.01 cm path length cell was used for obtaining the spectra. The CD spectra were signal-averaged by adding four scans, base-line-corrected, and smoothed. All the CD spectra were recorded at 25 °C. Peptide concentrations of 100 μM or less were used for obtaining CD spectra. Peptide−DMPC complexes for CD studies were prepared as follows. The appropriate volume of peptide solution was added to the DMPC MLVs to give a lipid to peptide molar ratio of 20:1. The mixture was incubated overnight at room temperature. This yielded an optically clear solution of the peptide−DMPC mixture.

The mean residue ellipticity, $[\Theta]_{MRE}$ (deg·cm^2·dmol^{-1}),was calculated using the equation:

$$[\Theta]_{MRE} = MRW\Theta/10cl$$

where MRW is the mean residue weight (molecular weight of the peptide divided by 18, the number of amino acids in the peptide), Θ is the observed ellipticity in degrees, c is the concentration of the peptide in grams per milliliter, and l is the path length of the cell in centimeters. The percent helicity of the peptide was estimated from the equation:

$$\% \ \alpha\text{-helix} = [([\Theta]_{222} + 3000)/(36000 + 3000)] \times 100$$

where, $[\Theta]_{222}$ is the mean residue ellipticity at 222 nm (Morrisett et al., 1973).

Differential Scanning Calorimetry (DSC). High-sensitivity DSC studies were performed in a Microcal MC-2 scanning calorimeter (MicroCal, Inc., Amherst, MA) at the scan rate of 20 deg h^{-1} at an instrumental sensitivity of 1 and with a filtering constant of 10 s. DMPC MLVs and DMPC MLV−peptide mixtures were prepared essentially as described above. The lipid to peptide molar ratios used in this study are 100:1 and 50:1. The suspension was degassed for 30 min before loading into the sample cell and run against buffer in the reference cell. Four consecutive scans from 8 to 38 °C with 60 min equilibration time between each scan were run for the same sample. No significant changes in the thermograms were observed for the first scan and the fourth scan. The observed transitions were analyzed using software (DA2, Version 2.1) provided by Microcal, Inc.

Fluorescence Measurements. Steady-state fluorescence emission spectra were recorded on an SLM 8100 spectrofluorometer (SLM Instruments, Inc., Urbana, IL) at 25 °C with constant magnetic stirring. A lipid to peptide molar ratio of 2000:1 with 0.5 μM peptide was used. Excitation and emission band-passes were 32 and 2 nm, respectively. An excitation wavelength of 280 nm was used, and emission spectra were recorded from 310 to 450 nm. For relative quantum yield measurements, the total area under the emission spectrum from 315 to 450 nm was integrated using the software provided by SLM Instruments, Inc. Quantum yields were determined relative to the quantum yield of NATA (ϕ = 0.15) (Kirby & Steiner, 1970). Relative quantum yields (ϕ) were calculated using the equation (Schiller, 1985):

$$\phi_{PP} = \phi_{AA}(I_{PP}A_{AA}/I_{AA}A_{PP})$$

where I is the fluorescence intensity and A is the absorbance. The subscripts PP and AA stand for the peptide and the standard, respectively.

For the determination of binding constants of the peptides with POPC SUVs, a 10 μL aliquot of a concentrated stock solution of the lipid (13 mM) was added to the peptide solution (0.5 μM). The emission spectra were recorded 2 min after addition of the lipid as described above. The contribution of scattered light to the observed signal was negligible under the experimental condition used. The binding isotherms were analyzed as partition equilibria using the formula:

$$X_b^* = K_p C_f$$

where X_b^* is the molar ratio of bound peptide per 60% of the total lipid (Beschiaschvili & Seelig, 1990; Gazit et al., 1995), K_p is the partition coefficient, and C_f is the free peptide concentration at equilibrium. The fraction of membrane-bound peptide (P_b) was calculated using the equation:

$$P_b = P_T(F - F_0)/(F_\infty - F_0)$$

where P_T is the total peptide concentration, F is thefluorescence intensity in the presence of POPC SUVs, F_∞ is the fluorescence intensity when all the peptide is membrane-bound, and F_0 is the fluorescence intensity in the absence of POPC. F_∞ was obtained from a double-reciprocal plot of F vs T_L (total lipid concentration) (Schwarz et al., 1986). Partition coefficients were obtained from the slopes of X_b^* vs C_f plots using the least-squares method (SigmaPlot, Version 1.02).

Acrylamide quenching experiments were performed using a 295 nm excitation wavelength. Aliquots (10 μL) of freshly prepared acrylamide (4 M) stock solutions were added to a 2.7 mL solution of either peptide alone or a lipid−peptide mixture. Corrections for inner-filter effects due to absorptive screening of acrylamide (ϵ_{295} = 0.25 M^{-1}cm^{-1}, for acrylamide) were made (Calhoun et al., 1983). The quenching data were analyzed according to the Stern−Volmer equation for collisional quenching (Eftink & Ghiron, 1981):

$$F_0/F = 1 + K_{sv}[Q] = \tau_0/\tau = 1 + k_q\tau_0[Q]$$

where F_0 and F are the fluorescence intensities in the absence and presence of quencher, respectively, K_{sv} is the Stern−Volmer constant for the collisional quenching process, [Q] is the quencher concentration, τ_0 and τ are the fluorescence lifetimes of the flurophore in the absence and presence of the quencher, respectively, and k_q is the bimolecular rate constant for the quenching process. The above equation predicts a linear plot of F_0/F (or τ_0/τ) vs [Q] for a homogeneously emitting solution.

Quenching studies with diBrPC (Markello et al., 1985; Killian et al., 1990; de Kroon et al., 1990, 1991; Johnson & Cornell, 1994; Ladokhin & Holloway, 1995) were carried out by incubating peptide (0.5 μM) with POPC SUVs with or without diBrPC (33 mol %) at a lipid to peptide molar ratio of 2000:1 overnight at room temperature. The emission

spectra were recorded as described above. The tryptophan position in the lipid bilayer was calculated by using the parallax method developed by Chattopadhyaya & London (1987):

$$Z_{1f} = [(1/-\pi C) \ln (F_1/F_2) - L_{21}^2]/2L_{21}$$

where Z_{1f} is the difference in shallower quencher and tryptophan depth, C is the quencher concentration (mole fraction/70 Å^2), F_1 and F_2 are the fluorescence intensities in the presence of shallower and deeper quencher, respectively, and L_{21} is the difference in depth of deeper and shallower quencher. F_1 and F_2 are obtained from the ratio of fluorescence intensity in the presence (F) and absence (F_0) of the respective quencher, i.e., $F_1 = F_1/F_0$ and $F_2 = F_2/F_0$. The distance of tryptophan from the bilayer center was calculated using the equation:

$$Z_{cf} = Z_{1f} + L_{c1}$$

where L_{c1} is the distance of the shallower quencher from the center of the bilayer.

RESULTS

Design and Synthesis of the Peptides. The distribution of charged amino acid residues in class A_1, class A_2, and class Y amphipathic helices present in different exchangeable apolipoproteins is compared using the program COMBO/QUALITY/SNORKEL (Jones et al., 1992; Segrest et al., 1994), and the results are shown in Figure 1. We designed and synthesized peptides Ac-18A_1-NH_2, Ac-18A_2-NH_2, and Ac-18Y-NH_2, which mimic the distribution of charged amino acid residues in class A_1, class A_2, and class Y amphipathic helices, respectively. Helical wheel representations (Schiffer & Edmundson, 1967) of sequences of the above three peptides are shown in Figure 2. The major features of the three peptides are as follows. (a) They all possess five leucine residues and a tryptophan residue on the nonpolar face of the helix. The tryptophan residue is located at the center of the nonpolar face and is the sixth residue from the N-terminal end in the linear sequence. Thus, the fraying of the helix termini is not expected to influence its properties. (b) The N- and C-terminal ends of the peptides are blocked by acetylation and amidation, respectively, to remove unfavorable charge−helix macrodipole interaction (Shoemaker et al., 1987; Fairman et al., 1989). Furthermore, it has been shown that end group blockage improves the lipid binding properties of a class A amphipathic helix and the end group blocked peptides mimic the properties of apolipoprotein A-I more closely compared to the unblocked peptide (Venkatachalapathi et al., 1993; Corijn et al., 1993). (c) All three peptides have four lysines and four glutamic acid residues and thus are zwitterionic at pH 7.4. (d) The first amino acid residue at the N-terminal end is glutamic acid in all three peptides whereas the C-terminal end is lysine in Ac-18A_1-NH_2 and Ac-18A_2-NH_2. The distribution of positively charged amino acid residues in class Y helices necessitated its positioning at the fifth position from the C-terminal end. The location of the negatively charged amino acid residue at the N-terminal end and the positively charged amino acid residue at the C-terminal end should further help in the stabilization of the helix (Forood et al., 1993).

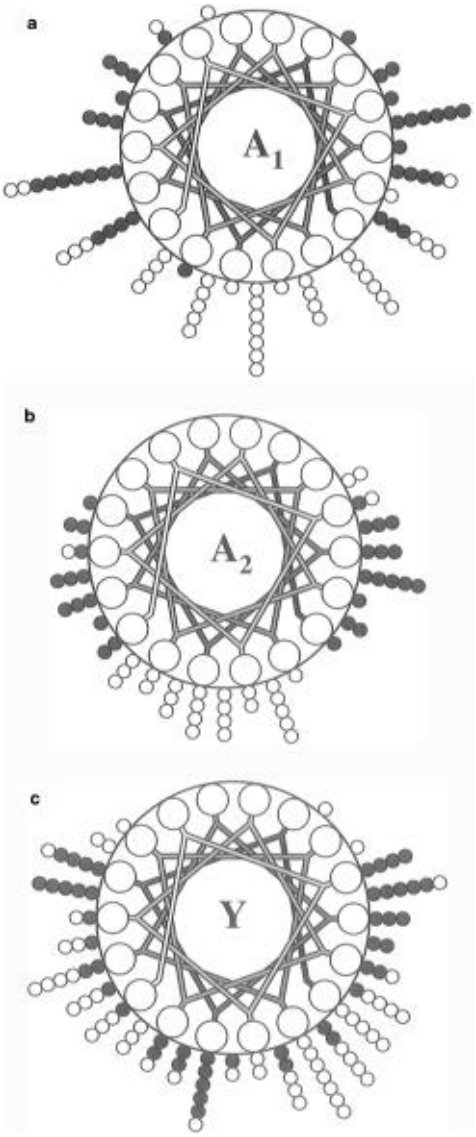

FIGURE 1: Distribution of charged amino acid residues in class A_1 (a), class A_2 (b), and class Y (c) amphipathic helices present in exchangeable apolipoproteins. Filled circles represent positive and open circles represent negative residues. The following sequences were analyzed: class A_1: apo A-I [44−65, 66−87, 121−142, 143−164, 165−186, 187−208], apo E [161−182, 203-266]; class A_2: apo A-II [7−30, 39−50, 51−71], apo C-I [7−32, 33−53], apo C-II [14−39, 44−55], apo C-III [40−67]; class Y: apo A-I [88−98, 99−120, 209−219, 220−241], apo A-IV [40−61, 62−94, 139−160, 183−204, 227−248, 249−288, 289−310, 311−332]. The above sequences were analyzed using COMBO/QUALITY/SNORKEL programs (Segrest et al., 1994). COMBO/QUALITY/SNORKEL is the sum of multiple WHEEL/SNORKEL analyses (Jones et al., 1992).

Reversed-Phase HPLC. Separation of the peptides on a RP-HPLC column is determined primarily by the hydrophobic interactions between the peptide and the acyl chains of the stationary phase of the column. RP-HPLC has been used successfully as a probe to study the secondary structure adopted by putative amphipathic helical peptides (Blondelle & Houghten, 1992; Aguilar et al., 1993; Mishra et al., 1995). It has been shown that peptides with a propensity to form amphipathic helix are induced into this structure upon binding to the stationary phase of the column (Blondell et al., 1993, 1995). It has also been shown that retention times of the amphipathic helical peptides are directly correlated with the length of the hydrophobic face of the helix (Blondell et al., 1993; Mishra et al., 1995). Among the three peptides, Ac-

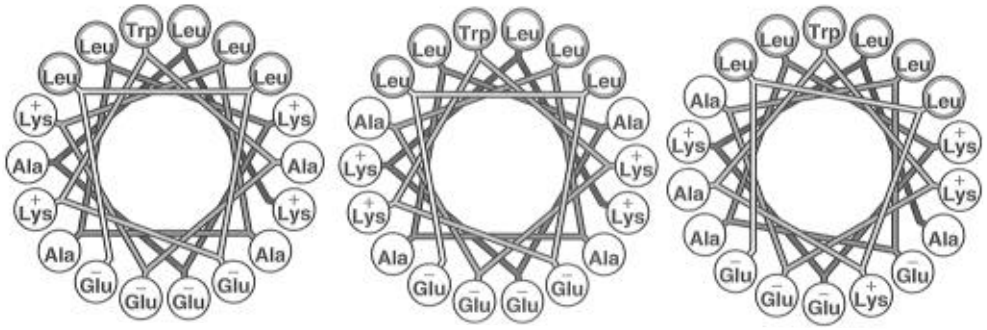

FIGURE 2: Helical wheel (Schiffer & Edmundson, 1967) representations of Ac-18A_1-NH_2 (a), Ac-18A_2-NH_2 (b), and Ac-18Y-NH_2 (c). Hydrophobic residues (except Ala) on the nonpolar face are shaded.

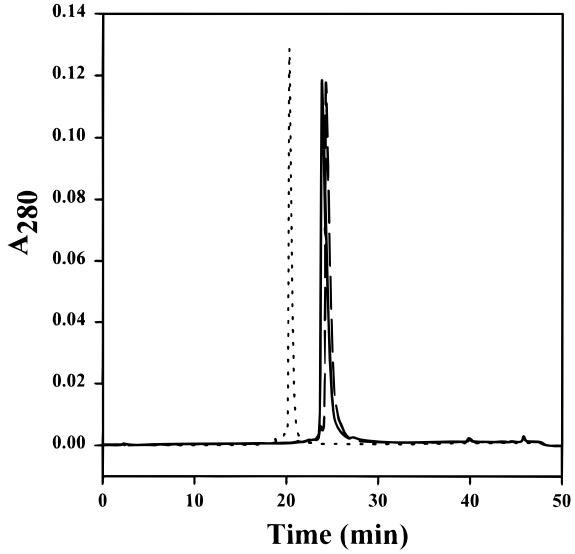

FIGURE 3: Analytical RP-HPLC profiles of Ac-18A_1-NH_2 (dotted line), Ac-18A_2-NH_2 (solid line), and Ac-18Y-NH_2 (dashed line). HPLC (Beckman System Gold) was done using a C-18 column (VYDAC, 4.6 mm i.d. × 25 cm, particle size 5 μm) and a linear gradient of 25−70% acetonitrile/water, containing 0.1% TFA, in 45 min.

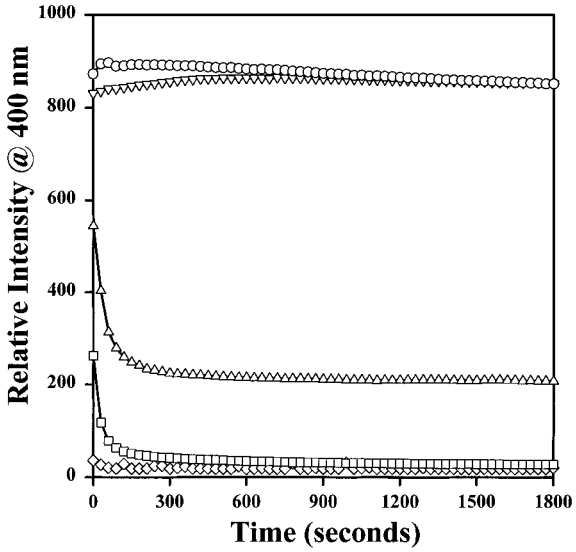

FIGURE 4: Right-angle light scattering measurements on DMPC MLVs and DMPC MLV−peptide mixtures. The lipid concentration was 200 μM, and the peptide concentration was 10 μM. The Triton X-100 concentration was 600 μM. The total volume of the mixture was 2.0 mL. All the measurements were carried out at 25 °C with constant magnetic stirring of the mixture using an SLM 8100 spectrofluorometer. Excitation and emission band-passes were 4 nm each. DMPC alone (▽), DMPC + Ac-18A_1-NH_2 (○), DMPC + Ac-18A_2-NH_2 (□), DMPC + Ac-18Y-NH_2 (△), DMPC + Triton X-100 (◇).

18A_1-NH_2 eluted earlier (retention time 20.3 min) than Ac-18A_2-NH_2 (23.8 min) and Ac-18Y-NH_2 (24.3 min) (Figure 3). This indicates that Ac-18A_1-NH_2 is the least hydrophobic among the three peptides.

The purity of the synthesized peptides as determined by analytical RP-HPLC on a C-18 column was ≥ 95% (Figure 3).

Right-Angle Light Scattering Measurements. Exchangeable apolipoproteins (Surewicz et al., 1986; Jonas et al., 1989) and their fragments (Vanloo et al., 1995; Palgunachari et al., 1996) as well as synthetic peptide analogs of exchangeable apolipoproteins (McLean et al., 1991; Corijn et al., 1993; Mishra et al., 1994) possess the ability to solubilize DMPC MLVs. The rate of solubilization of DMPC MLVs was monitored by measuring the decrease in scattered light intensity due to the vesicles after addition of the peptides (Surewicz et al., 1986; Venkatachalapathi et al., 1993; Mishra et al., 1994). The results are shown in Figure 4. At a lipid to peptide molar ratio of 20:1, Ac-18A_2-NH_2 showed the fastest rate of turbidity clarification followed by Ac-18Y-NH_2 (Figure 4). Although Ac-18A_1-NH_2 failed to solubilize the lipid vesicles during the time course of the experiment (Figure 4), it did so after overnight incubation of the peptide−lipid mixture at room temperature (data not shown). This indicates that the rate of association of Ac-18A_1-NH_2 with DMPC MLVs is slowest among the three peptides. As a positive control, Triton X-100 was added to the lipid vesicles. Complete solubilization of the vesicles occurred at a lipid to detergent molar ratio of 1:3 (Figure 4). The different rates of vesicle solubilization suggest that the difference in the distribution of charged amino acid residues in the three peptides has affected their rates of association with DMPC MLVs.

Secondary Structure of Peptides. The secondary structures of the three peptides under different environments were determined by CD spectroscopy. CD spectra of the three peptides in PBS are shown in Figure 5a. CD spectra of both Ac-18A_2-NH_2 and Ac-18Y-NH_2 show minima at 208 and 222 nm and a maximum at ~190 nm, characteristic of a right-handed α-helical conformation (Figure 5a) (Woody, 1995). The CD spectrum of Ac-18A_1-NH_2, however, shows

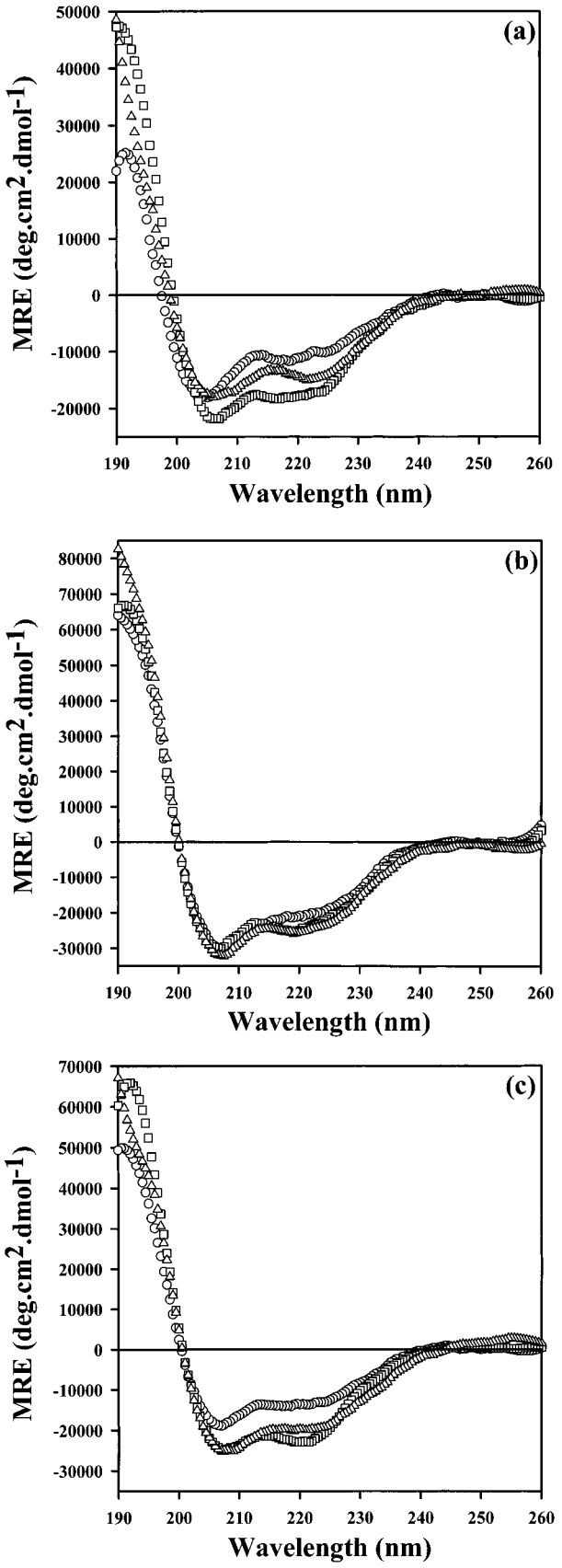

FIGURE 5: Far-UV CD spectra of the peptides in PBS (a), 50% (v/v) TFE (b), and DMPC (c) (lipid to peptide molar ratio 20:1). Peptide concentration was ~100 μM. All the spectra were recorded at 25 °C using a 0.01 cm cell on an AVIV 62DS spectropolarimeter. Four scans were collected, averaged, and smoothed using the software provided by AVIV. Ac-18A$_1$-NH$_2$ (○), Ac-18A$_2$-NH$_2$ (□), Ac-18Y-NH$_2$ (△).

minima at 205 and 218 nm and a maximum at 193 nm (Figure 5a). Moreover, the intensity of the band at 193 nm in the CD spectrum of Ac-18A$_1$-NH$_2$ is much reduced compared to the band at ~190 nm in the CD spectra of Ac-18A$_2$-NH$_2$ and Ac-18Y-NH$_2$ (Figure 5a). In addition, the zero crossover point (wavelength at which MRE is zero) in the CD spectrum of Ac-18A$_1$-NH$_2$ is shifted to shorter wavelength (197 nm) compared to Ac-18A$_2$-NH$_2$ (199.5 nm) and Ac-18Y-NH$_2$ (199 nm) (Figure 5a). Taken together, the above features of the CD spectrum of Ac-18A$_1$-NH$_2$ indicate that in PBS its helical content is lower compared to Ac-18A$_2$-NH$_2$ and Ac-18Y-NH$_2$. The MRE at 222 nm has been used to estimate helical contents in amphipathic peptides and proteins (Morrisett et al., 1973; Mishra et al., 1994, 1995). Based on the MRE at 222 nm, the helical contents of Ac-18A$_1$-NH$_2$, Ac-18A$_2$-NH$_2$, and Ac-18Y-NH$_2$ in PBS were estimated to be 34%, 52%, and 46%, respectively.

TFE has been shown to stabilize helical structures in shorter peptides (Sönnichsen et al., 1992; Jasanoff & Fersht, 1994; Waterhous & Johnson, 1994) as well as proteins (Shiraki et al., 1995). It has been shown that TFE stabilizes helical conformation by unfavoring H-bonding with the bulk solvent because of its lower basicity and thereby promoting intramolecular H-bonding (Sönnichsen et al., 1992; Zhou et al., 1993). TFE has also been shown to disrupt interhelical hydrophobic interactions because of its low dielectric constant (Lau et al., 1984). CD spectra of the three peptides in 50% TFE in PBS (v/v) are shown in Figure 5b. In this solvent, all three peptides show an increase in their helical content compared to PBS alone. The helical content is estimated to be 59%, 68%, and 70% for Ac-18A$_1$-NH$_2$, Ac-18A$_2$-NH$_2$, and Ac-18Y-NH$_2$, respectively. Thus, compared to their helical contents in PBS, in 50% TFE (v/v) the helical contents of the three peptides are quite similar. This is also evident by their CD spectra in this helix-stabilizing environment (Figure 5b).

Amphipathic lipid-associating peptides generally show an increase in their helicity in the presence of lipids compared to that in aqueous solution (McLean et al., 1991; Corijn et al., 1993; Mishra et al., 1994, 1995). The secondary structure of the three peptides in a lipid environment was investigated by recording their CD spectra in the presence of DMPC (Figure 5c). The helical contents of Ac-18A$_1$-NH$_2$, Ac-18A$_2$-NH$_2$ and Ac-18Y-NH$_2$, were estimated to be 43%, 66%, and 58%, respectively. Thus, in the presence of lipid, among the three peptides Ac-18A$_2$-NH$_2$ possesses the maximum helical structure (Figure 5c).

Differential Scanning Calorimetry. The effect of the three peptides on the thermotropic phase transition properties of DMPC MLVs was investigated by DSC at two different lipid to peptide molar ratios (100:1 and 50:1). Heating endotherms of DMPC MLVs and DMPC MLV−peptide mixtures at a lipid to peptide molar ratio of 100:1 are presented in Figure 6. DMPC MLVs show a pretransition at 13.0 °C and a gel to liquid-crystalline phase transition at 23.3 °C. These values are similar to those reported earlier (Lewis et al., 1987; Mishra et al., 1994, 1995). Addition of the peptides modified the phase transition properties of DMPC MLVs to different extents. All three peptides broadened the pretransition as well as the gel to liquid-crystalline phase transition. These effects are maximum in the case of Ac-18A$_2$-NH$_2$ and minimum in the case of Ac-18A$_1$-NH$_2$ (Figure 6). Association of the amphipathic helical peptides with DMPC MLVs often results in lowering of the transition enthalpy because of the disruption of the ordered lipid bilayer structure (Morrisett et al., 1977; McLean et al., 1990; Mishra et al.,

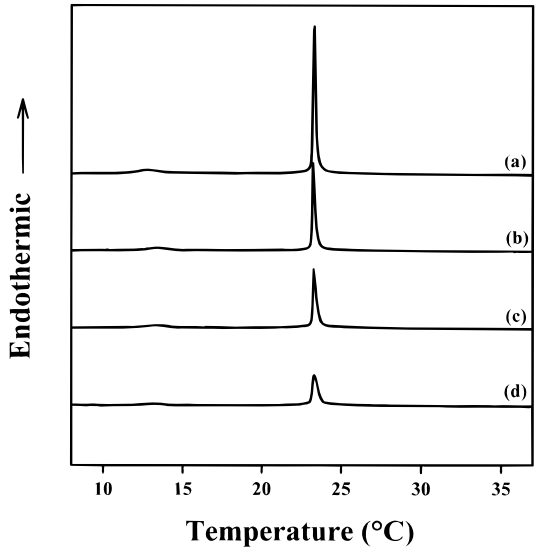

FIGURE 6: DSC heating endotherms of DMPC MLVs and DMPC MLV−peptide mixtures (lipid to peptide molar ratio was 100:1; lipid concentration was 1.5 mM). DSC studies were done using a Microcal MC-2 scanning calorimeter at a scan rate of 20 deg/h. Four scans from 8 to 38 °C were collected for each sample with 1 h equilibration time between each scan. For the same sample, no significant difference was observed between the scans. DMPC alone (a), DMPC + Ac-18A$_1$-NH$_2$ (b), DMPC + Ac-18Y-NH$_2$ (c), DMPC + Ac-18A$_2$-NH$_2$ (d).

Table 1: Effect of the Peptides on the Gel to Liquid-Crystalline Phase Transition of DMPC MLVs[a]

sample	T_m (°C)	ΔH_0 (kcal/mol)
DMPC	23.3	6.0
DMPC/Ac-18A$_1$-NH$_2$		
100:1[b]	23.2	5.0
50:1	23.3	4.5
DMPC/Ac-18A$_2$-NH$_2$		
100:1	23.3	3.6
50:1	23.3	3.2
DMPC/Ac-18Y-NH$_2$		
100:1	23.3	4.5
50:1	23.3	3.7

[a] DMPC concentration = 1.5 mM. T_m is the temperature at which the excess heat capacity is maximum, and ΔH_0 is the calorimetric enthalopy. [b] Lipid/peptide molar ratio.

1994, 1995). The enthalpy of the gel to liquid-crystalline phase transition (ΔH_0), measured as the area under the transition peak, was estimated in each case, and the values along with the transition temperature (T_m) are reported in Table 1. It is evident that the rank order of the three peptides in reducing the transition enthalpy at lipid to peptide molar ratios of 100:1 and 50:1 is Ac-18A$_2$-NH$_2$ > Ac-18Y-NH$_2$ > Ac-18A$_1$-NH$_2$ (Table 1). None of the peptides completely disrupted the bilayer structure as indicated by the invariance in the T_m of DMPC MLVs (Table 1).

Fluorescence Measurements. Fluorescence emission maxima and quantum yields are very sensitive to the microenvironment of tryptophan. A blue shift (movement to shorter wavelength) in the emission maximum accompanied by an increase in the quantum yield is generally observed when a tryptophan residue is transferred from a medium of high polarity to a medium of low polarity (Lakowicz, 1983; Schiller, 1985). To probe the microenvironment of tryptophan in the three peptides, their emission spectra were recorded in PBS and in the presence of POPC SUVs. The emission spectra are shown in Figure 7. As a control, emission spectra of NATA are also shown

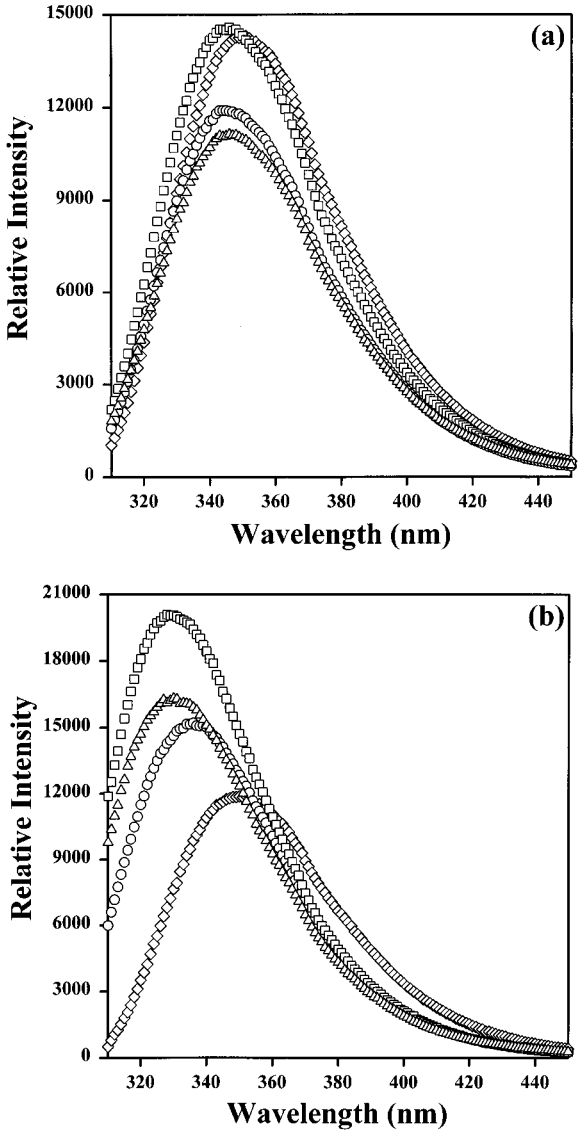

FIGURE 7: Fluorescence emission spectra of NATA and the peptides in PBS (a) and in the presence of POPC SUVs (b). Lipid to peptide molar ratio was 2000:1. Lipid concentration was 1.3 mM. All the spectra were recorded at 25 °C with constant magnetic stirring using an SLM 8100 spectrofluorometer. Excitation wavelength was 280 nm. Excitation and emission band-passes were 32 and 2 nm, respectively. Ac-18A$_1$-NH$_2$ (○), Ac-18A$_2$-NH$_2$ (□), Ac-18Y-NH$_2$ (△), NATA (◇).

Table 2: Fluorescence Properties and Partition Coefficients of the Peptides

	λ_{max} (nm)[a]		ϕ[b]		
peptide	PBS	POPC	PBS	POPC	K_p (M^{-1})[c]
Ac-18A$_1$-NH$_2$	345	336	0.12	0.14	2.0×10^3
Ac-18A$_2$-NH$_2$	345	328	0.15	0.17	11.1×10^3
Ac-18Y-NH$_2$	345	330	0.12	0.14	4.0×10^3
NATA	350	350	(0.15)[d]	0.12	ND[e]

[a] Wavelength of maximum emission. [b] Quantum yield relative to NATA. [c] Partition coefficient. [d] Quantum yield of NATA in water (Kirby & Steiner, 1970). [e] Not determined.

(Figure 7). The emission maxima and the relative quantum yields of the three peptides and NATA in buffer and in the presence of POPC SUVs are given in Table 2. All three peptides show a blue shift in the tryptophan emission maximum and an increased quantum yield in the presence of POPC SUVs compared to that in buffer (Figure 7, Table 2), indicating their interaction with POPC SUVs. Ac-18A$_2$-

NH_2 shows the largest (17 nm) whereas Ac-18A_1-NH_2 shows the smallest (9 nm) blue shift in the emission maximum in the presence of POPC SUVs compared to that in buffer (Table 2). The quantum yield of Ac-18A_2-NH_2 in the presence of POPC SUVs is also higher compared to Ac-18A_1-NH_2 and Ac-18Y-NH_2 (Table 2). There is no change in the emission maximum of NATA in the presence of POPC SUVs compared to that in PBS (Table 2). A decrease in the NATA quantum yield is observed in the presence of POPC SUVs compared to that in PBS (Table 2). The reason for this is not clear at present. The emission maxima and quantum yields indicate that, in the presence of POPC SUVs, the microenvironment of tryptophan in Ac-18A_2-NH_2 is most hydrophobic while the microenvironment of tryptophan in Ac-18A_1-NH_2 is least hydrophobic.

The increase in the tryptophan fluorescence intensity in the presence of POPC SUVs compared to that in buffer was utilized to evaluate the binding affinities of the three peptides for the lipid (Schwarz et al., 1986; Gazit et al., 1995). Small aliquots of a concentrated stock solution of POPC SUVs were added to peptide in PBS, and the resulting increase in the fluorescence intensity was plotted as a function of the lipid to peptide molar ratio (Figure 8a). These data were analyzed as described earlier (see Materials and Methods), and the resulting binding isotherms are shown in Figure 8b. The partition coefficient (K_p) of each peptide was estimated by extrapolating the initial slope of its binding curve to a zero equilibrium peptide concentration (C_f) value. The estimated partition coefficients for the three peptides are presented in Table 2. The data indicate that among the three peptides, Ac-18A_2-NH_2 has the highest while Ac-18A_1-NH_2 has the lowest partition coefficient (Table 2).

Since all three peptides contain a single tryptophan residue located at the center of the nonpolar face of the helix (Figure 2), the location of the tryptophan would give information about the depth of burial of the helix into the lipid bilayer. The location of tryptophan in the lipid bilayer was probed using both aqueous phase as well as membrane-resident quenchers. Acrylamide was used as an aqueous phase quencher (Eftink & Ghiron, 1981). Acrylamide is polar but uncharged and has good access to all but the most deeply buried tryptophan residues (Kurzban et al., 1989). Results of the quenching experiments in the form of Stern−Volmer plots are shown in Figure 9. As a control, quenching data of NATA are also included. A comparison of acrylamide quenching in PBS with that in the presence of POPC SUVs reveals that tryptophan residues in the three peptides are shielded in the presence of lipid compared to that in PBS (Figure 9a,b). This difference is more obvious if one compares acrylamide quenching of NATA and the three peptides in PBS *versus* that in the presence of POPC SUVs (Figure 9a *vs* Figure 9b). The Stern−Volmer quenching constants (K_{sv}) for the acrylamide quenching are presented in Table 3. The blue shift in the emission maximum, increased quantum yield, and shielding from acrylamide in the presence of POPC SUVs compared with that in PBS indicate that tryptophan residues in all three peptides are buried in the lipid bilayer.

To determine the depth of penetration of tryptophan in the POPC bilayer, quenching experiments with dibrominated lipids were carried out (Markello et al., 1985; Killian et al., 1990; de Kroon et al., 1990, 1991; Johnson & Cornell, 1994; Ladokhin & Holloway, 1995). The emission spectra of the three peptides and NATA, which served as a control, were

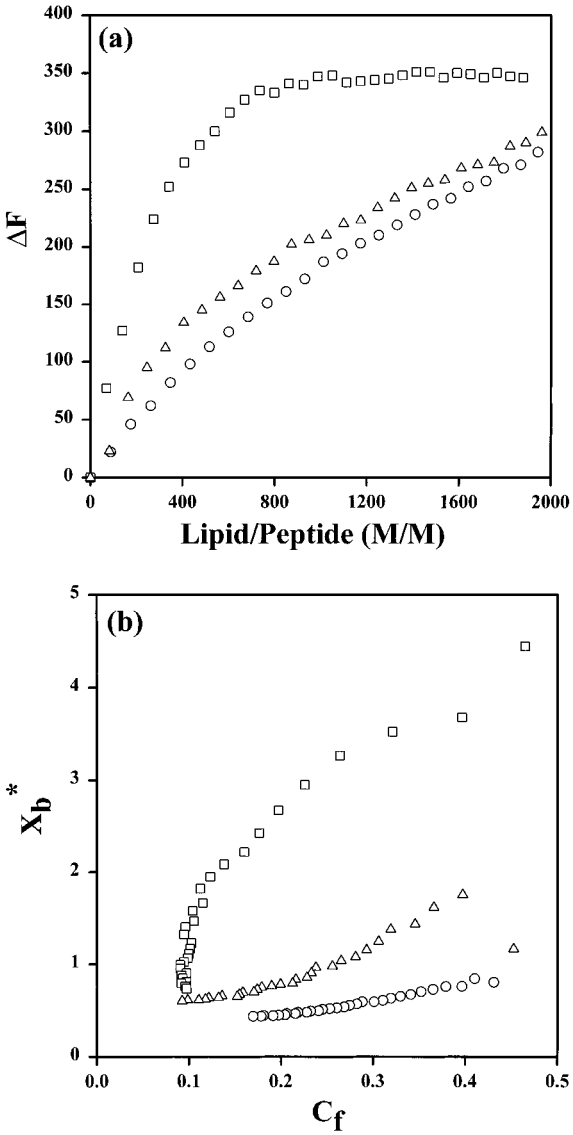

FIGURE 8: Increase in the fluorescence intensity of the peptide as a function of lipid to peptide molar ratio (a) and the resulting binding isotherm (b). X_b^* is the molar ratio of bound peptide per 60% of the total lipid, and C_f is the equilibrium free peptide concentration. A ~0.5 μM peptide solution was titrated with a stock solution of POPC SUVs (lipid concentration 13.1 mM). Other experimental conditions were the same as described for Figure 7. Ac-18A_1-NH_2 (○), Ac-18A_2-NH_2 (□), Ac-18Y-NH_2 (△).

recorded in the presence of POPC SUVs with or without 33 mol % dibrominated lipid. The quenching efficiency of each dibrominated lipid was calculated, and the results are shown in Figure 10. All three dibrominated lipids used (6,7-dibromo-PC, 9,10-dibromo-PC, and 11,12-dibromo-PC) were able to quench the fluorescence intensity of the three peptides to different extents. Among the three quenchers, however, 9,10-dibromo-PC was the most efficient quencher of Trp fluorescence of all three peptides (Figure 10). Quenching of NATA by the dibrominated lipids was minimal (Figure 10). Quenching by the three dibrominated lipids was used to calculate the location of the tryptophan residue in the peptide from the center of the lipid bilayer using the parallax method (Chattopadhyaya & London, 1987). The calculated distances for the three peptides are given in Table 3. It is evident that tryptophan residues in the three peptides are buried in the POPC bilayer to different extents: the tryptophan in Ac-18A_2-NH_2 is buried most deeply while the tryptophan in Ac-18A_1-NH_2 is buried least (Table 3). This

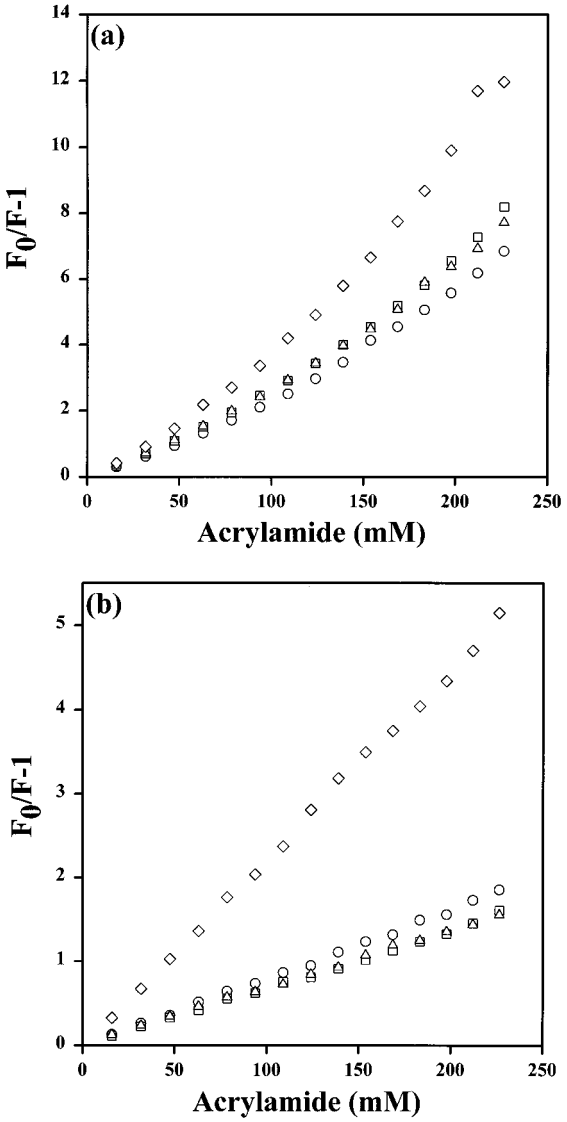

FIGURE 9: Stern−Volmer plots of fluorescence quenching by acrylamide of NATA and the peptides in PBS (a) and in the presence of POPC SUVs (b). Excitation wavelength was 295 nm. All other experimental conditions were the same as described for Figure 7. Ac-18A$_1$-NH$_2$ (○), Ac-18A$_2$-NH$_2$ (□), Ac-18Y-NH$_2$ (△), NATA (◇).

Table 3: Quenching Constants and Membrane Penetration Depths of the Peptides

peptide	K_{sv} (M^{-1})[a]		Z_{cf} (Å)[b]			Z_{cf} (Å)
	PBS	POPC	(1)[d]	(2)[e]	(3)[f]	(av)[c]
Ac-18A$_1$-NH$_2$	19.3	8.0	9.0	8.5	10.0	9.2
Ac-18A$_2$-NH$_2$	21.7	6.8	8.6	8.1	8.8	8.5
Ac-18Y-NH$_2$	22.5	6.8	8.9	8.7	9.3	9.0
NATA	28.1	22.3	ND[g]	ND	ND	ND

[a] Stern−Volmer quenching constant calculated as described under Materials and Methods. [b] Distance of tryptophan from the center of the POPC bilayer. [c] Average distance of tryptophan from the center of the POPC bilayer. [d] 6,7- and 11,12-diBrPC. [e] 6,7- and 9,10-diBrPC. [f] 9,10- and 11,12-diBrPC. [g] Not determined.

order is consistent with the observed blue shifts in the emission maxima and the partition coefficients of the three peptides in the presence of POPC SUVs (Table 2).

DISCUSSION

A detailed computer analysis of putative amphipathic α-helical segments in exchangeable apolipoproteins revealed

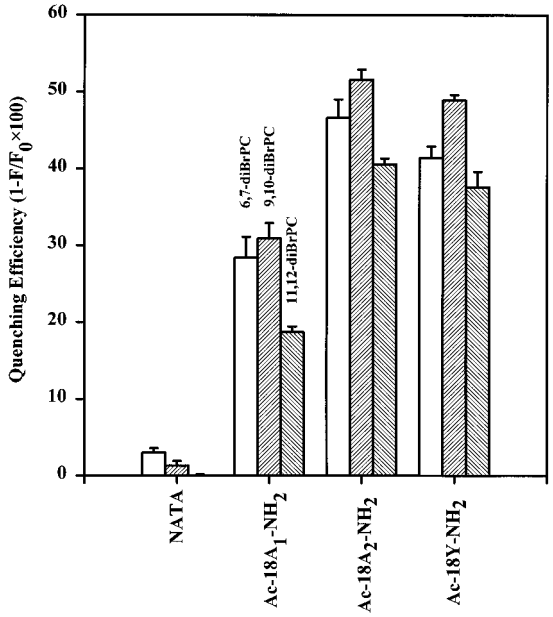

FIGURE 10: Quenching of NATA and the peptides by dibrominated lipids. Quenching efficiency was calculated as $(1 - F/F_0)100$, where F is the fluorescence intensity in the presence of POPC SUVs containing 33 mol % dibrominated lipid and F_0 is the fluorescence intensity in the presence of POPC SUVs without dibrominated lipid. Other experimental conditions were the same as described for Figure 7.

that the distribution of charged amino acid residues is different in different apolipoproteins (Segrest et al., 1992). To test the hypothesis that exchangeable apolipoproteins have different lipid affinity because of the presence of different classes of amphipathic α-helical motifs differing primarily in the distribution of charged amino acid residues, we designed and synthesized peptides Ac-18A$_1$-NH$_2$, Ac-18A$_2$-NH$_2$, and Ac-18Y-NH$_2$ (Figure 2). All three peptides have identical amino acid composition but differ in their primary amino acid sequence so as to mimic the distribution of charged amino acid residues in class A$_1$ (Ac-18A$_1$-NH$_2$), class A$_2$ (Ac-18A$_2$-NH$_2$), and class Y (Ac-18Y-NH$_2$) amphipathic helices present in exchangeable apolipoproteins (Figure 1). In the present study, we have studied the lipid-associating properties of the above three peptides.

The retention times of the three peptides on a C-18 RP-HPLC column indicated that, among the three peptides, Ac-18A$_2$-NH$_2$ is the most hydrophobic while Ac-18A$_1$-NH$_2$ is the least hydrophobic (Figure 3). Results of turbidity clarification indicated that Ac-18A$_2$-NH$_2$ also has the fastest rate of association with DMPC MLVs, while the rate of association of Ac-18A$_1$-NH$_2$ was slowest (Figure 4). In the presence of DMPC, Ac-18A$_2$-NH$_2$ has the maximum helical structure, while Ac-18A$_1$-NH$_2$ has the minimum helicity (Figure 5c). Among the three peptides, Ac-18A$_2$-NH$_2$ was most effective in reducing the enthalpy of the gel to liquid-crystalline phase transition of DMPC MLVs, while Ac-18A$_1$-NH$_2$ was least effective (Figure 6, Table 1).

In the presence of POPC SUVs, among the three peptides, Ac-18A$_2$-NH$_2$ showed the largest blue shift whereas Ac-18A$_1$-NH$_2$ showed the smallest blue shift in the emission maximum compared to that in PBS (Table 2). The partition coefficients for the three peptides indicated that among the three peptides, Ac-18A$_2$-NH$_2$ partitions most while Ac-18A$_1$-NH$_2$ partitions least in the POPC SUVs (Table 2). Acrylamide quenching studies indicated that in the presence of POPC SUVs, tryptophan in all three peptides is less

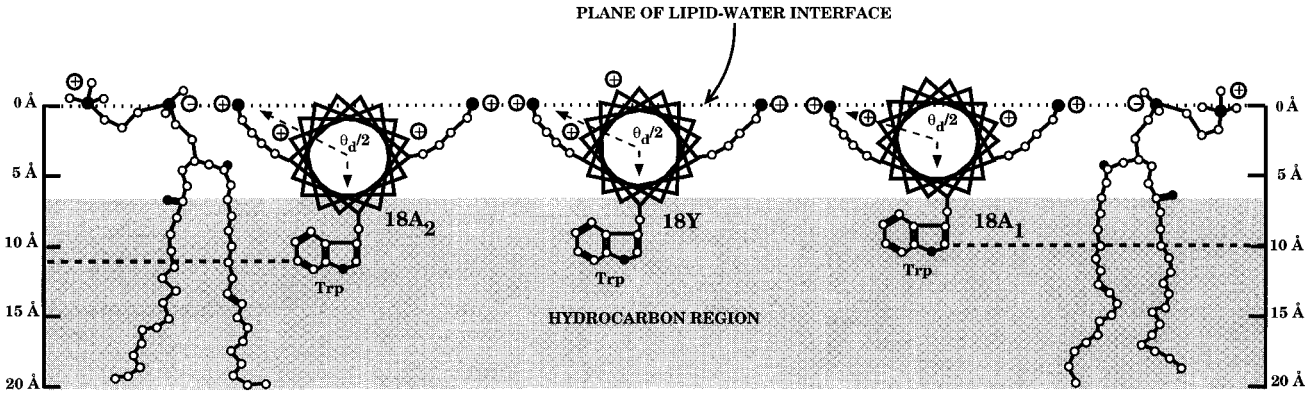

FIGURE 11: Schematic representation of depth of penetration of Ac-18A_1-NH_2 (18A_1), Ac-18A_2-NH_2 (18A_2), and Ac-18Y-NH_2 (18Y) in the POPC bilayer. The hydrocarbon region is assumed to start ~7 Å from the plane of the lipid−water interface (Palgunachari et al., 1996). The helices are represented in helical wheel projection showing two interfacial lysine residues in the snorkel orientation and the single tryptophan residue in each. The positions of the other two lysine residues in the peptides are indicated by (⊕) next to the helical wheel projection. The snorkel wedge angle (θ_d) (Palgunachari et al., 1996) for Ac-18A_1-NH_2, Ac-18A_2-NH_2, and Ac-18Y-NH_2 is 220°, 260°, and 240°, respectively.

accessible to the quencher than in PBS (Table 3). However, the accessibility of tryptophan in Ac-18A_1-NH_2 is more compared to the other two peptides (Table 3), indicating that it is buried less deeply in the bilayer.

The location of tryptophan residues of the three peptides in the POPC bilayer was further probed using dibrominated lipids (Markello et al., 1985; Killian et al., 1990; De Kroon et al., 1990, 1991; Johnson & Cornell, 1994; Ladokhin & Holloway, 1995). Dibrominated lipids were selected because the position of bromine atoms in the bilayers formed from these lipids has been determined by X-ray diffraction (McIntosh & Holloway, 1987; Weiner & White, 1991). Moreover, due to their small size, bromine atoms are least likely to perturb bilayer structure (Markello et al., 1985). Since DMPC has shorter lipid alkyl chains (C_{14}), it is not suitable for investigating the depth of penetration using dibrominated lipids. Among the three dibrominated lipids used, 9,10-diBrPC was the most effective while 11,12-diBrPC was the least effective quencher for all the three peptides (Figure 10). The quenching of tryptophan in Ac-18A_2-NH_2 was most while the quenching of tryptophan in Ac-18A_1-NH_2 was least with all three diBrPC used (Figure 10). This is consistent with the partitioning of Ac-18A_2-NH_2 being highest and the partitioning of Ac-18A_1-NH_2 being lowest in POPC SUVs (Table 2). The estimated distances of tryptophans from the center of the lipid bilayer for the three peptides indicate that among the three peptides, the tryptophan residue in Ac-18A_2-NH_2 is buried most deeply whereas the tryptophan in Ac-18A_1-NH_2 is buried least (Table 3). The penetration of the three peptides in the POPC bilayer is shown schematically in Figure 11.

Taken together, the above data indicate that among the three peptides, Ac-18A_2-NH_2 has the strongest while Ac-18A_1-NH_2 has the weakest lipid affinity. We have shown previously that interfacial lysine residues in a class A amphipathic helix, when associated with lipid, snorkel to bury their charge in the aqueous environment and thereby bury the nonpolar face of the helix deeper in the hydrophobic interior of the lipid monolayer (Mishra et al., 1994). Snorkeling of interfacial lysine residues has also been observed in class A_2 amphipathic helices of apo C-I when associated with SDS micelles by NMR spectroscopy (Rozek et al., 1995). Although it has been suggested that snorkeling of interfacial lysine residues may not be a universal phenomenon, the hydrophobic contribution of interfacial lysine residues has been shown to be important (Buchko et al., 1996). To explain the observed lipid affinity of synthetic amphipathic helical segments of apo A-I, we defined the snorkel wedge angle (θ_d) as the angle formed by the lysine residues nearest to and located on opposite sides of the center of the hydrophobic face on a helical wheel projection (Palgunachari et al., 1996). Each lysine residue used to define θ_d was assumed to contribute 40° to the angle (Palgunachari et al., 1996). Based on these assumptions, θ_d for Ac-18A_1-NH_2, Ac-18A_2-NH_2, and Ac-18Y-NH_2 is 220°, 260°, and 240°, respectively (Figure 11). Moreover, there are two more lysine residues contiguous to interfacial lysines in Ac-18A_2-NH_2 whereas there is only one lysine residue in Ac-18Y-NH_2 (Figure 2). These additional lysine residues will further broaden the hydrophobic faces of Ac-18A_2-NH_2 and Ac-18Y-NH_2, more so in the former than in the latter, compared to the hydrophobic face of Ac-18A_1-NH_2. Thus, the results of the present study can be explained based on the broadness of the hydrophobic face in the three peptides (Figure 11). We also suggest that in addition to increasing the width of the hydrophobic face, snorkeling of interfacial lysine residues also determines anchoring of the amphipathic helix in the lipid bilayer such that charges are optimally solvated.

As pointed out earlier, class A_2 amphipathic helices are present in apo A-II and apo Cs (C-I, C-II, and C-III). It has been shown that these apolipoproteins have higher lipid affinity compared to other exchangeable apolipoproteins which have either class A_1 helices (apo A-I and apo E) or class Y helices (apo A-I and apo A-IV) (Brausseur et al., 1992; Jonas, 1992). We have shown previously that in apo A-I, class Y helices have higher lipid affinity than class A_1 helices (Palgunachari et al., 1996). Thus, the results of the present study are in accord with these earlier observations.

To conclude, the results of this study emphasize the important role of interfacial lysine residues in increasing the lipid affinity of amphipathic helices. Furthermore, the results of this study indicate that the role of interfacial lysine residues in increasing the lipid affinity is additive. We propose that interfacial lysine residues also help anchor the amphipathic helix in the lipid bilayer.

ACKNOWLEDGMENT

We thank Professors G. M. Anantharamaiah and Jere P. Segrest for their invaluable help and encouragement for the

successful completion of the present work. We also thank Dr. Donald D. Muccio for the use of the spectropolarimeter.

REFERENCES

Aguilar, M. I., Mougos, S., Boublik, J., Rivier, J., & Hearn, M. T. W. (1993) *J. Chromatogr. 646*, 53−65.

Ames, B. N. (1966) *Methods. Enzymol. 8*, 115−118.

Anantharamaiah, G. M., Jones, M. K., & Segrest, J. P. (1993) in *The Amphipathic Helix* (Epand, R. M., Ed.) pp 109−142, CRC Press, Boca Raton, FL.

Beschiaschvili, G., & Seelig, J. (1990) *Biochemistry 29*, 52−58.

Blondell, S. E., & Houghten, R. A. (1992) *Biochemistry 31*, 12688−12694.

Blondell, S. E., Simpkins, L. R., Pérez-Paya, E., & Houghten, R. A. (1993) *Biochim. Biophys. Acta 1202*, 331−336.

Blondell, S. E., Ostresh, J. M., Houghten, R. A., & Pérez-Payá, E. (1995) *Biophys. J. 68*, 351−359.

Brasseur, R., Lins, L., Vanloo, B., Ruysschaert, J. M., & Rosseneu (1992) *Proteins: Struct., Funct., and Genet. 13*, 246−257.

Brouillette, C. G., & Anantharamaiah, G. M. (1995) *Biochim. Biophys. Acta 1256*, 103−129.

Buchko, G. W., Treleaven, W. D., Dunne, S. J., Tracey, A. S., & Cushley, R. J. (1996) *J. Biol. Chem. 271*, 3039−3045.

Calhoun, D. B., Vanderkooi, J. M., & Englander, S. W. (1983) *Biochemistry 22*, 1533−1539.

Chattopadhyay, A., & London, E. (1987) *Biochemistry 26*, 39−45.

Corijn, J., Deleys, R., Labeur, C., Vanloo, B., Lins, L., Brasseur, R., Baert, J., Ruysschaert, J. M., & Rosseneu, M. (1993) *Biochim. Biophys. Acta 1170*, 8−16.

de Kroon, A. I. P. M., Soekarjo, M. W., de Gier, J., & de Kruijff (1990) *Biochemistry 29*, 8229−8240.

de Kroon, A. I. P. M., de Gier, J., & de Kruijff (1991) *Biochim. Biophys. Acta 1068*, 111−124.

Eftink, M. R., & Ghiron, C. A. (1981) *Anal. Biochem. 114*, 199−227.

Fairman, R., Shoemaker, K. R., York, E. J., Stewart, J. M., & Baldwin, R. L. (1989) *Proteins: Struct., Funct., Genet. 5*, 1−7.

Forood, B., Feliciano, E. J., & Nambiar, K. P. (1993) *Proc. Natl. Acad. Sci. U.S.A. 90*, 838−842.

Gazit, E., Boman, A., Boman, H. G., & Shai, Y. (1995) *Biochemistry 34*, 11479−11488.

Jasanoff, A., & Fersht, A. R. (1994) *Biochemistry 33*, 2129−2135.

Johnson, J. E., & Cornell, R. B. (1994) *Biochemistry 33*, 4327−4335.

Johnson, W. C., Jr. (1990) *Proteins: Struct., Funct., Genet. 7*, 205−214.

Jonas, A. (1992) in *Structure and Function of Apolipoproteins* (Rosseneu, M., Ed.) pp 217−250, CRC Press, Boca Raton, FL.

Jonas, A., Kezdy, K. E., & Wald, J. H. (1989) *J. Biol. Chem. 264*, 4818−4824.

Jones, M. K., Anantharamaiah, G. M., & Segrest, J. P. (1992) *J. Lipid. Res. 33*, 287−296.

Killian, J. A., Keller, R. C. A., Struyvé, M., de Kroon, A. I. P. M., Tommassen, J., & de Kruijff, B. (1990) *Biochemistry 29*, 8131−8137.

Kirby, E. P., & Steiner, R. F. (1970) *J. Phys. Chem. 74*, 4480−4486.

Kurzban, G. P., Gitlin, G., Bayer, E. A., Wilchek, M., & Horowitz, P. M. (1989) *Biochemistry 28*, 8537−8542.

Ladokhin, A. S., & Holloway, P. W. (1995) *Biophys. J. 69*, 506−517.

Lakowicz, J. R. (1983) *Principles of Fluorescence Spectroscopy*, Plenum Press, New York.

Lau, S. Y. M., Taneja, A. K., & Hodges, R. S. (1984) *J. Chromatogr. 317*, 129−140.

Lewis, R. N. A. H., Mak, N., & McElhaney, R. (1987) *Biochemistry 26*, 6118−6126.

Markello, T., Zlotnick, A., Everett, J., Tennyson, J., & Holloway, P. W. (1985) *Biochemistry 24*, 2895−2901.

McIntosh, T. J., & Holloway, P. W. (1987) *Biochemistry 26*, 1783−1788.

McLean, L. R., Buck, S. H., & Krstenansky, J. L. (1990) *Biochemistry 29*, 2016−2022.

McLean, L. R., Hagaman, K. A., Owen, T. A., & Krstenansky, J. L. (1991) *Biochemistry 30*, 31−37 [see correction in (1991) *Biochemistry 30*, 11004].

Mishra, V. K., Palgunachari, M. N., Segrest, J. P., & Anantharamaiah, G. M. (1994) *J. Biol. Chem. 269*, 7185−7191.

Mishra, V. K., Palgunachari, M. N., Lund-Katz, S., Phillips, M. C., Segrest, J. P., & Anantharamaiah, G. M. (1995) *J. Biol. Chem. 270*, 1602−1611.

Morrisett, J. D., David, J. S. K., Pownall, H. J., & Gotto, A. M., Jr. (1973) *Biochemistry 12*, 1290−1299.

Morrisett, J. D., Jackson, R. L., & Gotto, A. M., Jr. (1977) *Biochim. Biophys. Acta 472*, 93−133.

Palgunachari, M. N., Mishra, V. K., Lund-Katz, S., Phillips, M. C., Adeyeye, S. O., Alluri, S., Anantharamaiah, G. M., & Segrest, J. P. (1996) *Arterioscler., Thromb., Vasc. Biol. 16*, 328−338.

Pownall, H. J., & Massey, J. B. (1982) *Biophys. J. 37*, 177−179.

Rosseneu, M., & Labeur, C. (1995) *FASEB J. 9*, 768−776.

Rozek, A., Buchko, G. W., & Cushley, R. J. (1995) *Biochemistry 34*, 7401−7408.

Schiffer, J., & Edmundson, A. B. (1967) *Biophys. J. 7*, 121−135.

Schiller, P. W. (1985) in *The Peptides* (Hruby, V. J., Ed.) Vol. 7, pp 115−164, Academic Press, San Diego, CA.

Schwarz, G., Stankowski, S., & Rizzo, V. (1986) *Biochim. Biophys. Acta 861*, 141−151.

Segrest, J. P., Jackson, R. L., Morrisett, J. D., & Gotto, A. M., Jr. (1974) *FEBS Lett. 38*, 247−253.

Segrest, J. P., de Loof, H., Dohlman, J. G., Brouillette, C. G., & Anantharamaiah, G. M. (1990) *Proteins: Struct., Funct., Genet. 8*, 103−117.

Segrest, J. P., Jones, M. K., de Loof, H., Brouillette, C. G., Venkatachalapathi, Y. V., & Anantharamaiah, G. M. (1992) *J. Lipid Res. 33*, 141−166.

Segrest, J. P., Garber, D. W., Brouillette, C. G., Harvey, S. C., & Anantharamaiah, G. M. (1994) *Adv. Protein. Chem. 45*, 303−369.

Shiraki, K., Nishikawa, K., & Goto, Y. (1995) *J. Mol. Biol. 245*, 180−194.

Shoemaker, K. R., Kim, P. S., York, E. J., Stewart, J. M., & Baldwin, R. L. (1987) *Nature (London) 326*, 563−567.

Sönnichsen, F. D., Van Eyk, J. E., Hodges, R. S., & Sykes, B. D. (1992) *Biochemistry 31*, 8790−8798.

Sparrow, J. T., & Gotto, A. M., Jr. (1980) *Ann. N.Y. Acad. Sci. 348*, 187−211.

Sparrow, J. T., & Gotto, A. M., Jr. (1982) *CRC Crit. Rev. Biochem. 13*, 87−107.

Stewart, J. M., & Young, J. D. (1984) *Solid Phase Peptide Synthesis*, Pierce Chemical Co., Rockford, IL.

Surewicz, W. K., Epand, R. M., Pownall, H. J., & Hui, S. W. (1986) *J. Biol. Chem. 261*, 16191−16197.

Vanloo, B., Demoor, L., Boutillon, C., Lins, L., Brasseur, R., Baert, J., Fruchart, J. C., Tartar, A., & Rosseneu, M. (1995) *J. Lipid Res. 36*, 1686−1696.

Venkatachalapathi, Y. V., Phillips, M. C., Epand, R. M., Epand, R. F., Tytler, E. M., Segrest, J. P., & Anantharamaiah, G. M. (1993) *Proteins: Struct., Funct., Genet. 15*, 349−359.

Waterhous, D. V., & Johnson, W. C., Jr. (1994) *Biochemistry 33*, 2121−2128.

Weisgraber, K. H. (1994) *Adv. Protein. Chem. 45*, 249−302.

Wiener, M. C., & White, S. H. (1991) *Biochemistry 30*, 6997−7008.

Woody, R. W. (1995) *Methods. Enzymol. 246*, 34−71.

Yang, J. T., Wu, C.-S. C., & Martinez , H. M. (1986) *Methods. Enzymol. 130*, 208−269.

Zhou, N. E., Kay, C. M., Sykes, B. D., & Hodges, R. S. (1993) *Biochemistry 32*, 6190−6197.

BI960760F